The Canadian Mineralogist
Vol. 39, pp. 319-330 (2001)

OLIVINE–LIQUID PARTITIONING OF VANADIUM AND OTHER TRACE ELEMENTS, WITH APPLICATIONS TO MODERN AND ANCIENT PICRITES

DANTE CANIL[§] AND YANA FEDORTCHOUK

School of Earth and Ocean Sciences, University of Victoria, P.O. Box 3055, Victoria, British Columbia V8W 3P6, Canada

ABSTRACT

The partitioning of V, Ti, Sc, Cr, Ni, Zn, Ga, Zr, La and Yb between olivine and coexisting basaltic and komatiitic liquids was measured at known fugacity of oxygen, $f(O_2)$. Olivine and glass were analyzed for trace elements using laser-ablation inductively coupled plasma – mass spectrometry (LA–ICP–MS). The purpose of the study was to further refine an empirical oxygen barometer for picritic magmas (>10% MgO) based on the comparison of the $f(O_2)$-dependent behavior of V with that of other incompatible and immobile trace elements (Ti, Sc, Ga, Zr and Yb) along the liquid line of descent. Results of this study present an improvement on the earlier estimates of redox conditions that utilized this approach because the partition coefficients for V and other incompatible trace elements (Ti, Sc, Ga, Zr and Yb) are measured in the same bulk-compositions under the same experimental conditions, eliminating any previous bias or correlations. The advantages and limits of the approach are demonstrated in applications to modern Hawaiian picrites, Archean komatiitic lavas and lunar rocks. Uncertainties in the method are significant [about ± 0.5 log $f(O_2)$ units], but it is applicable to mafic suites having an igneous phase-assemblage altered by metamorphism, or without a phase assemblage to which more conventional estimates of redox conditions can be applied. In many cases, crucial estimates of the minimum $f(O_2)$ can be made for many terrestrial and extraterrestrial rocks in the geological record.

Keywords: vanadium, olivine, basaltic liquid, partition coefficient, picrite, komatiite, oxygen fugacity.

SOMMAIRE

La répartition des éléments V, Ti, Sc, Cr, Ni, Zn, Ga, Zr La et Yb entre l'olivine et un bain fondu coexistant de composition basaltique ou bien komatiitique a été mesurée en fonction de la fugacité de l'oxygène, $f(O_2)$. Nous avons analysé l'olivine et le verre afin d'établir la concentration de ces éléments traces avec un appareil à plasma à couplage inductif avec ablation au laser, et par spectrométrie de masse. Le but de l'étude était d'affiner la détermination empirique antérieure de la pression d'oxygène dans les magmas picritiques (>10% MgO), fondée sur une comparaison du comportement du vanadium, qui dépend de la fugacité d'oxygène, et des autres éléments traces incompatibles et immobiles (Ti, Sc, Ga, Zr et Yb) lors d'une évolution du liquide au cours de la cristallisation. Ces résultats permettent une amélioration par rapport aux estimations antérieures des conditions de $f(O_2)$, dans lesquelles la même approche avait été utilisée. Dans cette approche, les coefficients de partage pour le vanadium et autres éléments traces incompatibles (Ti, Sc, Ga, Zr et Yb) sont évalués en utilisant les mêmes compositions globales sujettes aux mêmes conditions expérimentales, éliminant ainsi tout traitement biaisé et les fausses corrélations. Nous démontrons les avantages et les limitations de cette approche avec une application aux suites récentes de picrites hawaiiennes, aux laves komatiitiques archéennes et aux roches lunaires. Les incertitudes associées à cette méthode ne sont pas négligeables [environ ± 0.5 log $f(O_2)$], mais en revanche elle peut s'appliquer à une suite de roches mafiques dans laquelle l'assemblage de minéraux ignés à subi les effets d'un métamorphisme, ou bien dans laquelle l'assemblage de phases nécessaire pour une évaluation plus conventionnelle de la fugacité d'oxygène est absente. Dans plusieurs cas, il est possible d'obtenir une estimation importante de la fugacité minimum d'oxygène de suites de roches terrestres et extraterrestres.

(Traduit par la Rédaction)

Mots-clés: vanadium, olivine, liquide basaltique, coefficient de partage, picrite, komatiite, fugacité d'oxygène.

§ *E-mail address*: dcanil@uvic.ca

INTRODUCTION

As an early-crystallizing phase on the liquidus of mafic and ultramafic magmas, olivine plays a central role in the compositional evolution of basaltic magmas along their liquid line of descent (Bowen 1928). It is in this context that the calibration and application of the Fe–Mg exchange equilibrium between olivine and liquid so elegantly developed by Roeder & Emslie (1970) has become a cornerstone in igneous petrology. Since that study, numerous other investigators have further implemented olivine–liquid equilibria for trace elements to monitor intensive and extensive variables in magmatic systems. This approach has been well explored for the partitioning of divalent cations in olivine (Hart & Davis 1978, Hirschmann & Ghiorso 1994, Snyder & Carmichael 1992, Takahashi 1978). The database with which to study and apply the incorporation of heterovalent cations into the olivine structure is more limited (Beattie 1994, Colson *et al.* 1988, Kennedy *et al.* 1992).

The distribution of V between olivine and liquid has been used to decipher the fugacity of oxygen, $f(O_2)$, during crystallization of komatiitic magmas related by olivine sorting, but whose primary mineralogy has been modified by subsequent metamorphism, thus eliminating the application of more conventional oxygen barometers (Canil 1997). This approach could also find additional applications in modern fresh basaltic or picritic lavas devoid of glass or Fe–Ti oxides for oxygen barometry. In this study, we present results of additional experiments designed to investigate the partition of V and other trace elements with changing $f(O_2)$ in a wider compositional space, at elevated pressure, and in some critical experiments at trace element levels. The new experimental data allow refinement of an olivine–liquid oxygen barometer based on V partitioning, and provide further insights into the incorporation of heterovalent elements into the olivine structure. Some applications to suites of both modern and ancient picrites are attempted to test the validity and limits of this oxygen barometer for terrestrial and extraterrestrial magmas.

BACKGROUND

The partition of V into the liquidus phases of mafic and ultramafic magmas shows increasing promise as an oxygen barometer for application to mantle melts and residues (Canil 1997, 1999, Canil & Fedortchouk 2000). The basis for using V abundances as an oxygen barometer is as follows. Vanadium is a polyvalent cation in magmas, existing in four potential valence states (V^{2+}, V^{3+}, V^{4+} and V^{5+}: Borisov *et al.* 1988). At terrestrial values of $f(O_2)$, V exists principally as V^{3+} or V^{4+} in magmas (Borisov *et al.* 1988). In previous work on V partitioning in olivine (Fig. 1), spinel (Canil 1999) and clinopyroxene (Canil & Fedortchouk 2000), the values of $D_V^{crystal/liq}$ scale to $f(O_2)$ by a factor of 0.25, requiring that the following redox equilibrium:

$$VO_{1.5} + 0.25O_2 = VO_2 \quad (1)$$

with

$$K = \frac{a_{VO_2}}{a_{VO_{1.5}} \cdot f(O_2)^{0.25}} \quad (2)$$

(where a is activity) operates in melts and governs the crystal–liquid partition. The abundance of V^{4+} is small in melts, but the proportion of V^{3+}, and thus the V^{3+}/V^{4+} ratio, decreases substantially with increasing $f(O_2)$. The crystal structures of most phases on the liquidus of mafic and ultramafic magmas prefer to incorporate V^{3+}, and for this reason bulk $D_V^{crystal/liq}$ (which includes $D_{V3+}^{crystal/liq}$, $D_{V4+}^{crystal/liq}$) decreases with increasing $f(O_2)$. A redox couple showing similar behavior in magmas is Cr^{2+}/Cr^{3+}, which also decreases with increasing $f(O_2)$ (Barnes 1986, Roeder & Reynolds 1991, Schreiber & Haskin 1976).

The V oxygen barometer for olivine–liquid is based on the variation in partition coefficient $D_V^{ol/liq}$ with $f(O_2)$, and its effect on the covariations of V with other trace elements preserved in any sequence of igneous rocks related by olivine sorting (fractionation or accumulation), whether they be fresh or metamorphosed. Any post-eruptive change of V^{3+}/V^{4+} is irrelevant. The sequence of rocks need only be a closed system with respect to its bulk abundance of V to preserve the redox memory during differentiation. The partition of most non-transition trace elements into crystallizing olivine is independent of $f(O_2)$ (see below). Because the ratio V^{3+}/V^{4+} in melts depends on $f(O_2)$, the availability of V^{3+} to partition into olivine changes with this variable, thus affecting the covariation of V with Ti, Sc, Zr and Yb along the liquid line of descent of a magma crystallizing olivine.

This approach in oxygen barometry for suites of ultramafic rock (Canil 1997) was originally based on the results of experiments at elevated levels of V. Although Henry's Law behavior was demonstrated, it was done over a fairly restricted compositional range. The study by Canil (1997) also originally applied only to komatiitic magmas, and the calibration was not carried out further into more common basalt compositions. In addition, Canil (1997) relied on published values for $D_{Ti}^{ol/liq}$, $D_{Sc}^{ol/liq}$, $D_{Yb}^{ol/liq}$, *etc.*, to compare with experimentally derived $D_V^{ol/liq}$ in order to constrain $f(O_2)$. This may have added some bias to that approach, because $D_V^{ol/liq}$ may be correlated with $D_{Ti}^{ol/liq}$, $D_{Sc}^{ol/liq}$, $D_{Yb}^{ol/liq}$, *etc.*, by coupled substitutions affecting the olivine structure (Beattie 1994). In principle, to evaluate these possible coupled substitutions, experimental data on all element partitions (*i.e.*, V with Ti, Sc, Zr, Yb) in the same experiment and composition should be measured.

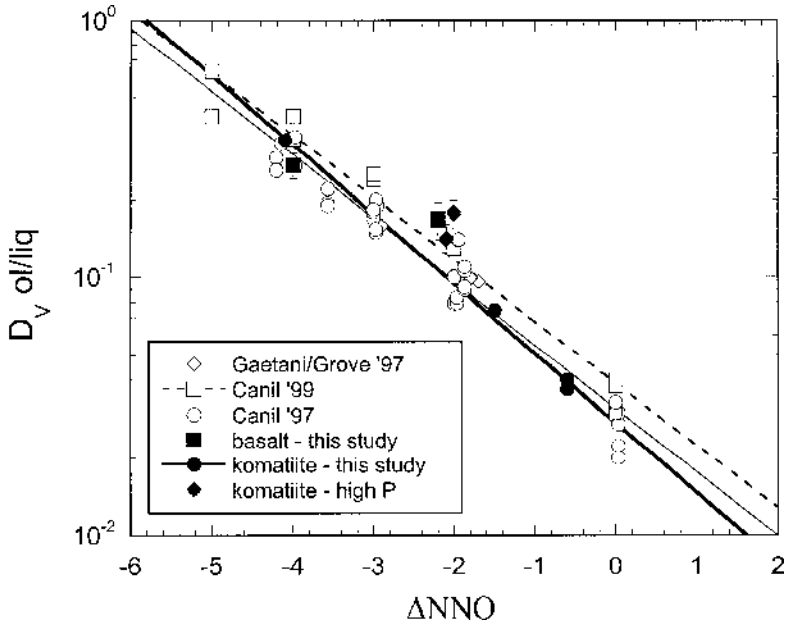

FIG. 1. Correlation of $D_V^{ol/liq}$ with $f(O_2)$ relative to the nickel – nickel oxide buffer (ΔNNO = log$f(O_2)$ sample – log$f(O_2)$ NNO buffer at P, T of interest). Open symbols are from previous studies on komatiite (Canil 1997, 1999, Gaetani & Grove 1997), and filled symbols are results from this study. Note that the results on komatiite and basalt in this study are similar to previous work within error (1σ). The new experiments on komatiite involving vanadium at trace levels are fit to an equation: logD_V = –0.24(±0.01)ΔNNO – 1.41(±0.06), r^2 = 0.99 (thick line), that is within error of all previous work at enhanced levels of V: logD_V = –0.23(±0.02)ΔNNO – 1.46(±0.05), r^2 = 0.95 (thin line). Uncertainties in regressions are expressed at a 2σ level. Note that the slope of the line in both datasets is within error of the value of 0.25 expected from the redox equilibrium $VO_{1.5}$ + 0.25O_2 ⇔ VO_2.

Finally, the effects of pressure on $D_V^{ol/liq}$ have not been explicitly evaluated or investigated by experiment, but they may play a role in extension of this technique to magmas crystallizing at greater depths (*cf.* Canil 1999).

METHODS

Basalt and komatiite were used as starting compositions (Table 1). A synthetic Hawaiian tholeiitic basalt (htbv) glass from the study of Webb & Dingwell (1990) was doped with V_2O_5 and used in two experiments to examine the effect of composition on $D_V^{ol/liq}$. In addition, two bulk compositions corresponding to Al-depleted and Al-undepleted komatiites (auk1, adk1, respectively) were synthesized and doped with V, Ti, Sc, Ni, Ga, Yb, La, Zn, Zr and Ge. Synthetic glasses of these compositions were synthesized by mixing reagent-grade $CaCO_3$, MgO, SiO_2, Al_2O_3 Fe_2O_3, $ZnCO_3$, Ni metal and V_2O_5 in an agate mortar. These mixtures were decarbonated at 900°C, fused into glasses in a Pt crucible at 1500°C in air in a box furnace, and reground in an agate mortar. The oxides La_2O_3, Yb_2O_3, Sc_2O_3, GeO_2, Ga_2O_3 and ZrO_2 were then added in <1 wt% amounts to the mixture, which was then reground in an agate mortar, fused a second time for 24 hours, and ground to a powder. The final mixture was doped with 2 wt% Cr_2O_3 to ensure that the melt was saturated with chromian spinel.

Experiments at 100 kPa were performed in a Deltech DT–31–V–OT vertical tube furnace over a range of $f(O_2)$ from that of air to 4 units below the nickel – nickel oxide buffer (*i.e.*, NNO–4) at temperatures of 1175° to 1375°C (Table 2). Temperature was measured with a Pt–$Pt_{90}Rh_{10}$ thermocouple calibrated at the melting point of gold. Oxygen fugacity was controlled to ±0.1 log$f(O_2)$ units by CO–CO_2 gas mixing and measured during each experiment with a solid zirconia electrolyte cell.

For the 100 kPa experiments, the powders of starting materials were mixed with ethyl alcohol, mounted as a slurry on 0.15 mm diameter Pt wire loops, and then sintered with a torch. To avoid Fe loss, the Pt loops were

TABLE 1. STARTING COMPOSITIONS, EXPERIMENTS ON PARTITIONING OF VANADIUM BETWEEN OLIVINE AND LIQUID

	auk1	adk1	hlbv	komvcr
Na_2O wt%			2.48	
MgO	19.4	20.1	7.3	24.6
Al_2O_3	9.4	5.87	13.5	7.6
SiO_2	44.5	48.7	51.2	45.2
CaO	9.9	9.8	10.5	7.4
TiO_2	0.61	0.60	2.58	b.d.
V_2O_5	0.21	0.19	0.59	0.8
Cr_2O_3	a.d.	a.d.	0.02	1.1
MnO			0.17	b.d.
FeO*	9.3	9.4	10.8	12.8
NiO	0.36	0.35	b.d.	b.d.
total**	93.68	95.01	99.14	99.50
V ppm	1401	1198		
Sc	436	436		
Ni	3198	2941		
Zn	94	54		
Ga	517	458		
Ge		4		
Zr	2716	2709		
La	8076	7696		
Yb	9212	8913		

Major-element concentrations, expressed as oxides, were determined by EMP. Concentrations of the other elements were determined by LA ICP MS. Data for komvcr are taken from Canil (1999).
* All Fe is expressed as FeO.
** Total for auk1 and adk1 glasses does not include doped trace elements; 2 wt% Cr_2O_3 added after glass synthesis to ensure spinel saturation.
b.d.: below detection, a.d.: element added after glass synthesis.

TABLE 2. CONDITIONS FOR PARTITIONING EXPERIMENTS

sample	Temp (°C)	$\log f(O_2)$	ΔNNO	time
132adk1	1375	-6.6	−0.6	28
133auk1	1375	−10.1	−4.1	22
135auk1	1375	−7.4	−1.5	28
132 auk1	1375	−6.6	-0.6	28
129adk1	1375	−0.68	6.6	48
dt18 hlbv	1175	−12	4.0	48
dt19 hlbv	1175	−10.2	−2.2	48
pe94-6 komvcr*	1525		−2.1	24
pe93 4 komvcr*	1425		−2.0	24

All experiments at 100 kPa except pe94-6 and pe93-4, which were run at 1 GPa.
* ΔNNO calculated using equations (3) and (4) in text. Run duration in hours.

presaturated with the rock composition at the desired T–$f(O_2)$ conditions for 24 h, quenched, and the glass dissolved in HF. A new mixture was sintered to the Fe-presaturated Pt loop, and used again at identical T–$f(O_2)$ conditions for the final experiment. For each experiment, the Pt loops were hung within ~3 mm of the thermocouple, introduced to the gas furnace above the liquidus, and the furnace sealed until the desired $f(O_2)$ was achieved. The sample was then cooled within seconds to the liquidus temperature, and further cooled at a rate of 1°C/h to the final run temperature with a programmable temperature controller. The liquidus and final temperatures for these compositions differ by only 25°C. The latter step was carried out to grow large crystals for subsequent analysis for the trace elements of interest. The crystallization interval did not produce any significant compositional heterogeneity in the olivine. At the end of the experiment, the Pt loops were quickly removed from the furnace and quenched in a stream of air.

Additional experiments were performed at 1 GPa on a komatiite composition (komvcr) in an end-loaded piston–cylinder apparatus at the Bayerisches Geoinstitut, Germany, using assemblies 19 mm in diameter with talc–pyrex pressure media and tapered graphite furnaces. Temperature was measured with a Pt–$PtRh_{10}$ thermocouple with no correction for pressure on EMF. A –10% friction correction was applied on the basis of a pressure calibration (von Seckendorff & O'Neill 1993). For each experiment, the starting material was loaded into a graphite-lined Pt capsule, dried overnight in a vacuum oven, and welded shut. The sample was pressurized, heated to the liquidus, held for 5 minutes, and then cooled at 6°C/h with programmable temperature controller to the final temperature of the experiment. After the desired run-duration, the experiment was quenched by terminating power to the furnace.

In the piston–cylinder experiments, $f(O_2)$ cannot be strictly controlled in graphite-lined Pt capsules, but was monitored by loading a 30-μm Pt wire into both the komatiite capsule and an adjacent capsule containing a synthetic harzburgite composition in the same experiment. At the conditions of these experiments, the harzburgite composition forms an assemblage of olivine + orthopyroxene + melt. The Fe content of the Pt wire and the compositions of coexisting olivine and orthopyroxene allow $f(O_2)$ in the experiment to be estimated by the equilibrium (Rubie *et al.* 1993):

$$Fe + O_2 + SiO_2 \Leftrightarrow Fe_2SiO_4 \quad (3)$$

in Pt ol

with a_{SiO2} in the system calculated using the equilibrium:

$$Mg_2Si_2O_6 \Leftrightarrow Mg_2SiO_4 + SiO_2 \quad (4)$$

opx ol

In the komatiite charge, no orthopyroxene is present, but its composition is calculated from olivine using the experimentally measured $K_{DFe-Mg}^{ol/opx}$ (von Seckendorff & O'Neill 1993). Results for Pt wires in both the komatiite and peridotite charges produced similar estimates of $f(O_2)$, even though a_{SiO2} is not buffered in the orthopyroxene-free komatiite experiments (Table 2).

Products of experiments were mounted in epoxy, sectioned, polished and examined in reflected light. Major-element compositions of crystals, Pt wire and glass were measured using a JEOL JXA 8900R electron microprobe (EMP) at the University of Alberta, with a 5-μm beam, operated at 20 kV, 20 nA. Analytical conditions were 10 s on peaks for all major elements, 60 s for Cr and Ni, and 100 s for V. Natural and synthetic standards were used for calibration, and the data were reduced with a ZAF procedure. Ten analyses of both crystal and glass were made in each run product, and the results were averaged (Table 3). No EMP analyses were performed on the run product of the one experiment in air (129 adk).

The concentrations of V, Ti, Sc, Ni, Ga, Zr, Yb, La, Zn and Ge in coexisting olivine and glass were determined by laser-ablation inductively coupled plasma – mass spectrometry (LA–ICP–MS) at the University of Victoria. We used a Merchantek Geolase™ LUV266 Nd –YAG UV laser coupled to a VG™ PlasmaQuad IIS ICP–MS quadrupole instrument. Full details of the instrumentation, calibration, analytical procedures and off-line data reduction are given elsewhere (Canil & Fedortchouk 2000, Chen 1999). Precision and accuracy are better than 5% and 10%, respectively, for all elements except Sc and Ti (better than 30%), on the basis of replicate analyses of standard glass of BCR–2 basalt (Chen *et al.* 2000). For each run product, three or more spots on the glass and coexisting olivine crystals were analyzed. The quality of the analysis is sample-dependent. In a few cases, the analytical signal for olivine was influenced by interference from small grains of chromian spinel or melt inclusions, or by crystal thickness. These effects could be filtered out in off-line data-signal reduction and were not important for most elements, but in two experiments, melt inclusions likely contributed to the high La signal in olivine (Table 4). Uncertainties reported for each analysis in Table 4 represent one standard deviation from the mean result of *n* analyses of glass or crystal, where *n* is the number of analytical results used in the average.

TABLE 3 CHEMICAL COMPOSITION OF EXPERIMENTAL RUN PRODUCTS*

sample	Na_2O	MgO	Al_2O_3	SiO_2	CaO	TiO_2	V_2O_3	Cr_2O_3	MnO	FeO	NiO	total**
132adk1 gl	b.d.	19.6	6.6	51.9	9.8	0.51	0.26	0.33	b.d.	9.6	0.15	98.9
		0.09	0.04	0.12	0.05	0.01	0.02	0.01		0.05	0.01	
132adk1 ol	b.d.	50.4	0.03	40.6	0.24	0.00	b.d	0.15	b.d.	7.8	0.74	100.1
		0.17	0.02	0.16	0.02	0.00		0.02		0.06	0.05	
133auk1 gl	b.d.	19.2	11.4	49.8	10.5	0.55	0.26	0.29	b.d.	7.0	0.01	99.2
		0.09	0.06	0.12	0.07	0.04	0.02	0.02		0.08	0.01	
133auk1 ol	b.d.	51.5	0.07	40.8	0.25	0.01	b.d.	0.18	b.d.	6.7	0.04	99.6
		0.23	0.03	0.11	0.02	0.02		0.01		0.22	0.04	
135auk1 gl	b.d.	16.6	10.9	47.2	10.6	0.55	0.39	0.27	b.d.	9.4	0.12	98.7
		0.16	0.11	0.21	0.08	0.02	0.05	0.02		0.03	0.01	
135auk1 ol	b.d.	50.1	0.07	40.4	0.24	b.d.	b.d.	0.15	b.d.	8.05	0.72	99.8
		0.31	0.01	0.19	0.01			0.02		0.09	0.10	
132 auk1 gl	b.d.	18.8	10.8	48.1	10.1	0.54	0.25	0.25	b.d.	9.5	0.16	98.7
		0.07	0.03	0.08	0.07	0.02	0.02	0.02		0.01	0.00	
132 auk1 ol	b.d.	50.9	0.08	40.8	0.25	b.d.	b.d.	0.14	b.d.	7.7	0.67	100.6
		0.23	0.02	0.39	0.01			0.01		0.11	0.03	
dt18 htbv gl	2.12	5.15	15.8	50.7	10.6	2.93	0.48	0.00	0.12	9.9	0.01	97.9
	0.07	0.09	0.11	0.36	0.26	0.08	0.04	0.00	0.03	0.34	0.01	
dt18 htbv ol	b.d.	37.5	b.d	38.3	0.56	0.09	0.13	0.01	0.26	23.7	0.04	100.7
		0.54		0.23	0.07	0.02	0.01	0.01	0.04	0.47	0.03	
dt19 htbv gl	2.28	4.78	15.9	50.4	10.3	2.91	0.48	0.00	0.09	9.7	0.01	97.0
	0.10	0.09	0.13	0.67	0.15	0.06	0.05	0.01	0.03	0.37	0.01	
dt19 htbv ol	b.d.	38.3	b.d.	37.4	0.62	0.10	0.08	0.02	0.28	24.3	0.05	101.4
		0.46		0.40	0.10	0.04	0.01	0.02	0.06	0.52	0.03	
94-6 komver gl	0.02	19.5	9.3	48.1	9.4	0.05	0.91	0.84	0.03	9.8	0.00	98.2
	0.01	0.32	0.19	0.27	0.11	0.02	0.09	0.06	0.03	0.35	0.00	
94-6komver ol	b.d.	50.5	b.d.	40.4	0.21	0.00	0.13	0.36	0.03	10.0	0.03	101.8
		0.44		0.31	0.01	0.01	0.01	0.06	0.03	0.33	0.03	
93-4 komver gl	0.05	16.9	10.0	48.0	10.2	0.06	0.85	0.56	0.03	12.0	0.00	98.8
	0.02	0.14	0.12	0.34	0.07	0.02	0.09	0.05	0.02	0.28	0.01	
93-4 komver ol	b.d.	48.1	b.d.	37.9	0.28	0.00	0.15	0.30	0.02	13.7	0.02	100.5
		0.27		0.26	0.02	0.01	0.01	0.09	0.02	0.24	0.02	

* Each row lists average results of at least 10 analyses of olivine (ol) and coexisting glass (gl) for each experiment, followed by a row listing standard deviations (1σ). Results are quoted in wt%.
** Glass totals are low in some cases because all Fe is listed as FeO*, and Fe_2O_3 has not been considered. b.d.: below detection.

TABLE 4. CONCENTRATIONS OF TRACE ELEMENTS AND DISTRIBUTION COEFFICIENTS

sample	135 auk1	135 auk1	132 auk1	132 auk1	132 adk1	132 adk1	133 auk1	133 auk1	129 adk1	129 adk1
phase	ol	gl	ol	gl	ol	gl	ol	gl	ol	gl
n	3	3	3	3	3	3	1	1	1	3
V	206(94)	1295(14)	64(27)	1333(156)	59(5)	1388(33)	386	1133	4.19	1020(1)
Sc	54(8)	328(15)	49(19)	342(6)	51(12)	368(7)	56	272	47	321(8)
TiO_2	0.022(9)	0.400(19)	0.011(4)	0.395(45)	b.d.	0.426(7)	0.010	0.334	0.01	0.37(1)
Ni	3107(295)	476(26)	2675(217)	800(161)	2765(243)	817(186)	237	79	6177	1238(31)
Zn	10(5)	2(1)	7(1)	4(1)	8	5	7	2	96	99.0(7)
Ga	6(2)	19(2)	7(3)	119(25)	4(1)	154(8)	b.d.	1	3	306(8)
Zr	67(57)	1821(106)	22(34)	2035(358)	3(1)	2334(125)	2	1474	1.1	1870(69)
La	181(158)*	4798(329)	49(80)*	5592(1375)	0.6(1)	6442(399)	0.47	4053	0.25	5269(207)
Yb	260(108)	5361(391)	158(86)	6503(1930)	143(25)	7685(603)	120	4422	112	6030(265)
D_V	0.16(7)		0.05(2)		0.040(1)		0.34		0.004(1)	
D_{Sc}	0.16(3)		0.14(6)		0.14(3)		0.21		0.146(3)	
D_{Ti}	0.06(2)		0.03(1)		n.d.		n.d.		0.024(1)	
D_{Ni}	6.5(7)		3.34(73)		3.38(83)		2.99		5(1.2)	
D_{Zn}	5(2)		1.75(27)		1.60(8)		3.5		0.97(1)	
D_{Ga}	0.3(1)		0.055(1)		0.025		n.d.		$9.8(2)\times10^{-3}$	
D_{Zr}	$3.7(3)\times10^{-2}$		$1.1(7)\times10^{-2}$		$1.2(4)\times10^{-5}$		1.35×10^{-3}		$6(1)\times10^{-4}$	
D_{La}	*		*		$9.9\ (0.6)\times10^{-5}$		1.17×10^{-4}		$4.20(18)\times10^{-5}$	
D_{Yb}	0.049(20)		0.024(15)		0.019(4)		0.027		0.079(1)	

Uncertainties at the 1σ level for the last digits reported given in brackets. * These results have too high a level of La in olivine owing to intersection of glass inclusions during analysis. Other elements were not affected. Symbols: ol: olivine, gl: glass, b.d.: below detection limit, n.d.: not determined.

RESULTS

Vanadium partitioning in olivine

Five experiments were carried out at 100 kPa and 1375°C on the komatiite compositions auk1 and adk1 to investigate the partitioning of V between olivine and liquid at trace levels. Exceptionally large crystals of olivine, in some cases up to 1 mm in size, were produced in these experiments. No zoning could be recognized in either trace- or major-element analysis of the olivine. These experiments also were saturated in chromian spinel (Table 2), which appeared both as inclusions in the olivine grains and as individual grains surrounded by glass. The composition of the chromian spinel is the subject of a much larger study on spinel–liquid equilibria and will be reported elsewhere.

The results of these experiments show a dependence of $D_V^{ol/liq}$ on $f(O_2)$ that is indistinguishable within error of results of previous studies (Fig. 1) over a range of temperatures from 1225° to 1425°C in five different bulk-compositions ranging from komatiite to chondrite (Canil 1997, 1999, Gaetani & Grove 1997, Kennedy *et al.* 1992). The data at both NNO – 2 and NNO – 4 from this and previous studies show that Henry's Law is obeyed for V in olivine and melt up to levels of at least 0.8 and 2.5 wt%V_2O_3, respectively (Fig. 2).

Two experiments at 100 kPa and 1175°C on the tholeiitic basalt composition htbv produced smaller crystals of olivine and no coexisting chromian spinel. The $D_V^{ol/liq}$ values for these experiments are identical within error to those for the komatiite compositions (Fig. 1). The two high-pressure experiments at 1 GPa on komatiite komvcr produced one large crystal of olivine and one crystal of chromian spinel set in glass. The results for $D_V^{ol/liq}$ on this composition are indistinguishable from those observed in komatiitic melts at 100 kPa,

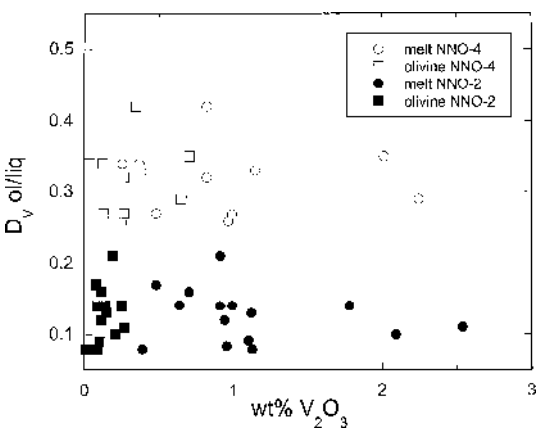

FIG. 2. Plot showing the lack of change in $D_V^{ol/liq}$ with V concentration in both olivine and melt in experiments at NNO – 4 and NNO – 2 (Canil 1997, 1999, Gaetani & Grove 1997). These results show that Henry's Law is obeyed to levels of at least 0.5 wt% and 2.5 wt% V_2O_3 in olivine and melt, respectively.

considering the uncertainties of ±0.3 log units in the $f(O_2)$ estimate using the Fe content of Pt wires in these experiments (equation 3). Thus, increased pressure at constant $f(O_2)$ does not significantly affect the $D_V^{ol/liq}$ *versus* $f(O_2)$ correlation. Suzuki & Akaogi (1995) also reported no pressure effect on $D_V^{ol/liq}$ in komatiite, peridotite and olivine bulk-compositions at more extreme pressures (to 14 GPa), but these experiments were performed using Li-doped charges (to facilitate heterovalent substitutions in olivine), and $f(O_2)$ was not monitored.

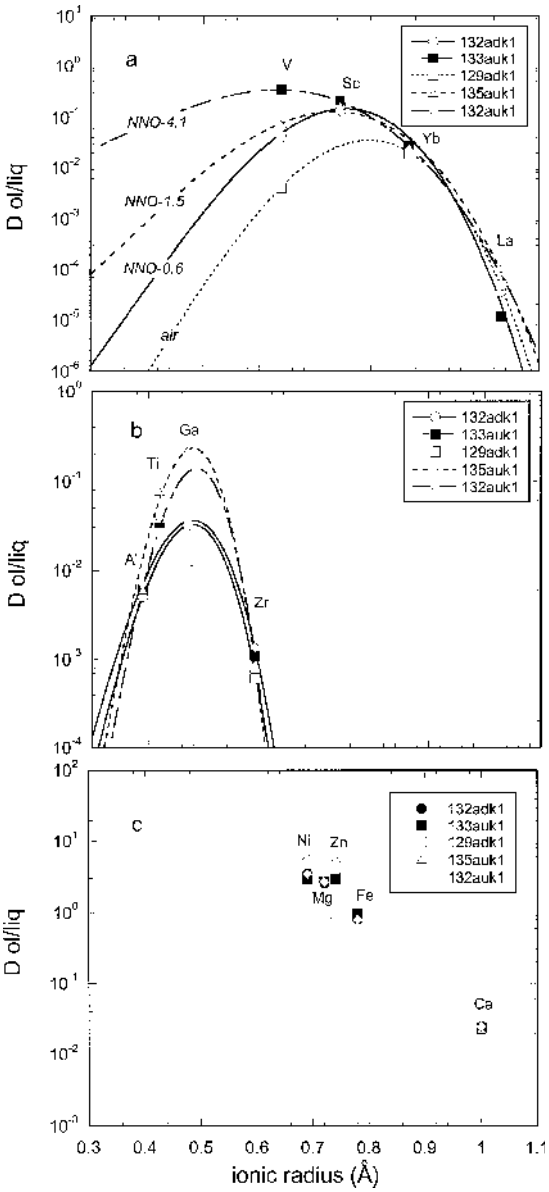

FIG. 3. Correlation of $D_{element}^{ol/liq}$ measured in this study with ionic radius (Shannon 1976) of (a) trivalent cations at *M* sites, (b) cations at *T* sites and, (c) divalent cations at *M* sites in olivine. The data are fit using a lattice-strain model (Blundy & Wood 1994) according to equation (5) in the text. The fit parameters are listed in Table 5.

Partitioning of other trace elements in olivine

The partitioning of Ti, Sc, Cr, Ni, La, Yb, Zr , Ga, Zn and Ge between olivine and liquid also was measured in the experiments at 1375°C and 100 kPa on the komatiite bulk-compositions auk1 and adk1 (Table 4). No data for $D_{Ge}^{ol/liq}$ could be obtained because this element was lost by volatilization during preparation of the starting composition. There are significant mass-fractionation effects involved in the determination of Zn concentrations by LA–ICP–MS (Chen 1999), such that results for $D_{Zn}^{ol/liq}$ should be viewed with caution. If one assumes that the fractionation effects during analysis of olivine and coexisting glass are the same during LA–ICP–MS analysis, the partition coefficient (which measures their ratio) should be valid.

Results for the trace-level experiments are compared in plots of $D_{element}^{ol/liq}$ *versus* ionic radius. The trends for trivalent, divalent and tetravalent cations (Fig. 3) all show the expected parabolic dependence consistent with crystal-structure constraints being the major factors controlling the partitioning of these elements into olivine (Blundy & Wood 1994, Onuma *et al.* 1968). At a given P–T–*X* condition, the *D* values for different cations D_i (P,T,*X*) in Figure 3 were fitted by weighted, non-linear regression to an equation of the form:

$$D_i(P, T, X) = D_o(P, T, X) \times \exp\left[\frac{-4\pi E N_A\left[\frac{r_o}{2}(r_i - r_o)^2 + \frac{1}{3}(r_i - r_o)^3\right]}{RT}\right] \quad (5)$$

where N_A is Avogadro's number, T is temperature (in K), E is the lattice-site Young's modulus (in kbar), D_o (P,T,*X*) describes the strain-free substitution of a cation with optimum ionic radius (r_o) for the site, and r_i is ionic radius of the substituent cation (Blundy & Wood 1994). In equation (5), D_i and r_i are known, and the fit parameters E, D_o and r_o, obtained from the regressions of experimental data (Table 5), describe in a general way the width, peak and location of the peak, respectively, of the parabola in Figure 3 (Wood & Blundy 1997).

The lattice-strain approach generally produced very good fits to the experimental data where $D^{ol/liq}$ for more than three cations were available. Certain assumptions improved fitting procedures. The *M*2 and *M*1 sites in olivine were considered to be fully disordered and to

TABLE 5. FIT PARAMETERS FOR LATTICE-STRAIN MODELING*

Experiment	D_o	E GPa	r_o Ångströms
		Trivalent cations at *M* site	
132adk1	0.150(3)	44.9(5)	0.7560(9)
133auk1	0.341(1)	21.2(2)	0.634(1)
129adk1	0.035(1)	45.6(5)	0.7971(5)
135auk1	0.131(2)	31.8(4)	0.734(1)
		Tetrahedral (*T*) site	
132adk1	0.032(2)	202(21)	0.479(5)
133auk1	0.139(1)	290(4)	0.48591)
135auk1	0.233(2)	302(3)	0.478(4)
132auk1	0.036(9)	176(22)	0.479(3)
		Divalent cations at *M* site	
132adk1	2.83(1)	31.5(2)	0.7570(6)
132auk1	2.98(2)	32.3(2)	0.7588(7)

* The 2σ uncertainties in fit parameters (given in brackets) are from weighted multiple regression of experimental data to equation (5) in text. Fit parameters for some experimental datasets are not reported because less than three datapoints were available (Table 4) or because they did not converge during the regression.

have identical elastic properties. In addition, Al^{3+}, Ga^{3+} and Ti^{4+} were considered to substitute into the tetrahedral rather than octahedral site in olivine, owing to the negative correlation of the proportion of these cations with that of Si in the olivine (Table 2). The values for $D_{Cr}^{ol/liq}$ are not plotted, but do not follow the trend for trivalent or divalent cations in Figure 3, possibly because of crystal-field effects (Suzuki & Akaogi 1995). Crystal-field effects were not considered to have a large influence on V because it fits the trend for partitioning of trivalent cations.

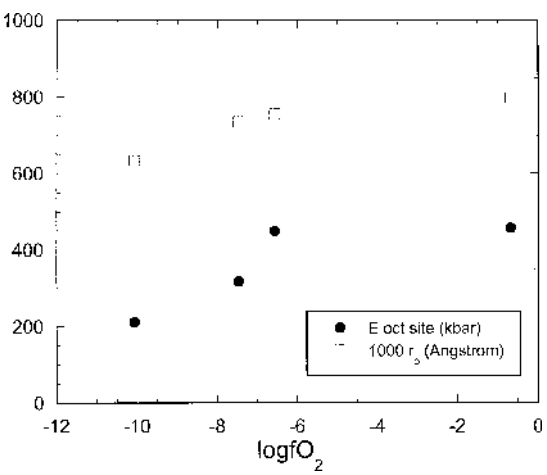

FIG. 4. Positive correlation of $f(O_2)$ with the site-defined Young's modulus (E, kbar) and optimal radius (r_o, Ångström units) parameters derived from lattice strain modeling (Table 5) for heterovalent substitution at the *M* site of olivine (data from this study).

The results from lattice-strain modeling show some systematic crystallographic information about the response of the olivine structure to changes in composition and $f(O_2)$ and its role in V partitioning. For a trivalent ion substituting at the octahedral site, the *D* parabola generally widens and shifts to the right with increasing $f(O_2)$ (Fig. 3a). With increasing $f(O_2)$, incorporation of V^{3+} cations at the octahedral site occurs with larger strain (represented by increasing E), and the optimum radius r_o increases, probably owing to changes in Fo content of olivine and concomitant larger metal–O distances at the *M* sites (Fig. 4).

A comparison of $D_{element}^{ol/liq}$ values from this study with previous work by Beattie (1994) and Kennedy *et al.* (1992) for the same elements is shown in Figure 5a. $D_{element}^{ol/liq}$ values are similar for most elements except Ti and Zr, which are higher by a factor of 2 to 4 in the current experiments. When considered together, all results show that $D_V^{ol/liq}$ has no strong correlation with $D_{element}^{ol/liq}$ for Ti, Sc, Yb or Zr (Fig. 5a). The values of $D_{element}^{ol/liq}$ for the latter elements vary by at most a factor of two among the various studies compared to order-of-magnitude changes in $D_V^{ol/liq}$ (Fig. 5a). The lack of any observable correlation in $D_V^{ol/liq}$ with $D_{Ti,Sc,Yb,Zr}^{ol/liq}$ is critical in the applications of trace element partitioning for Mg-rich olivine and liquid to be developed further below.

APPLICATIONS

The pattern of distribution of any element along the liquid line of descent in any crystallizing magma is controlled by the phases appearing on the liquidus. Olivine and chromian spinel are the only two phases to crystallize on the liquidus of magmas with greater than 10% MgO, with the exceptions of high-Mg boninites, which crystallize orthopyroxene (Francis 1995). During the accumulation or removal of olivine crystals in picritic magmas, the covariation of V with Ti, Sc, Ga and Yb along their liquid line of descent can be affected by magma redox conditions because of the change in $D_V^{ol/liq}$ with essentially little or no change in $D_{Ti,Sc,Yb,Ga}^{ol/liq}$ with $f(O_2)$ (Fig. 5a). If olivine control is assumed or demonstrated to be the only process responsible for geochemical variations in a given suite of picrite, then the slopes on plots of (Ti, Sc, Ga, Yb)/V *versus* V reflect the relative compatibility of these elements during olivine sorting. As an example, Figure 6 shows the different covariations for Ti, Sc, Yb, Ga and Lu with V in a suite of exceptionally well-characterized picrites from the Mauna Kea shield intersected in the Hawaii Scientific Drillhole that show compositional variation attributed to olivine control (Rhodes 1996, Yang *et al.* 1996). The positive correlations of Lu, Ga, Ti and Yb with V

in this suite indicate that $D_V^{ol/liq}$ is greater than $D_{Lu,Ga,Ti,Yb}^{ol/liq}$, whereas the negative correlation implies that $D_V^{ol/liq}$ is less than $D_{Sc}^{ol/liq}$. A zero correlation between V and any element would mean that $D_V^{ol/liq}$ is approximately equal to $D_{element}^{ol/liq}$ during differentiation. If the lava compositions in this suite reflect only olivine sorting, then the relationship $D_{Lu}^{ol/liq} < D_V^{ol/liq} < D_{Sc}^{ol/liq}$ holds, with an $f(O_2)$ estimated to be a maximum of NNO – 1 and a minimum of NNO – 3.5 using the constraints shown schematically in Figure 5b.

In examining the covariation of V with Ti, Sc, Yb and Zr in picrite suites to constrain $f(O_2)$, it is prudent to consider the role of chromian spinel, a common inclusion in early-formed phenocrysts of magnesian olivine, on the abundances of these elements. In the Mauna Kea lavas (Fig. 6), chromian spinel occurs as inclusions in olivine phenocrysts (Baker *et al.* 1996), and it is clear from Cr distributions in this suite that this mineral was part of the fractionating assemblage. In Mg-rich magmas at terrestrial values of $f(O_2)$, V is very compatible in chromian spinel ($D_V^{ol/liq} > 2$) (Canil 1999), and significant removal or addition of even small amounts of this phase could greatly affect the abundance of this element along a liquid line of descent. The covariation of Ti with V in the suite of Mauna Kea picrites is modeled in Figure 6 to show how addition of chromian spinel to the fractionating assemblage can change the $f(O_2)$ estimated by V partitioning. The covariation of Ti and V along the liquid line of descent can be modeled by crystal fractionation and accumulation of 100% olivine at

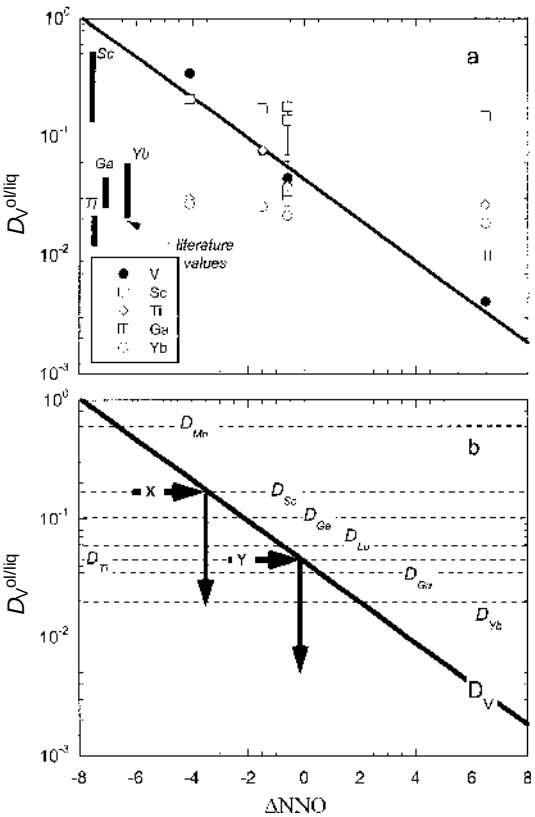

FIG. 5. (a) Plot showing the general lack of correlation between $D_V^{ol/liq}$ and $D_{element}^{ol/liq}$ for Ga, Yb, Ti and Sc measured in this study (symbols in legend). The thick line shows the dependence of $D_V^{ol/liq}$ with $f(O_2)$ from Figure 1. Also shown for comparison are the range of literature values (vertical bars) measured for $D_{Ga,Yb,Ti,Sc}^{ol/liq}$ (Beattie 1994, Kennedy *et al.* 1992). (b) Comparison of $D_V^{ol/liq}$ (thick line) and $D_{Mn,Sc,Ge,Lu,Ti,Ga,Yb}^{ol/liq}$ (dashed lines) as a function of $f(O_2)$. The thick arrows show how $f(O_2)$ can be bracketed by comparison of the D values required to explain the covariation of any element with V along a liquid line of descent in a picrite suite related by olivine sorting. For example, if V behaves more incompatibly than Sc (negative slope for Sc/V *versus* V, $D_V^{ol/liq} < D_{Sc}^{ol/liq}$) but more compatibly than Ti (positive slope for Ti/V *versus* V, $D_V^{ol/liq} > D_{Ti}^{ol/liq}$), then the $f(O_2)$ during differentiation must be between NNO – 3.5 (arrow "X") and NNO – 0.5 (arrow "Y"). Better-constrained estimates of $f(O_2)$ can be made where the two elements covarying with V in a picrite suite have more similar compatibility in olivine (*e.g.*, Lu, Ti and Ga).

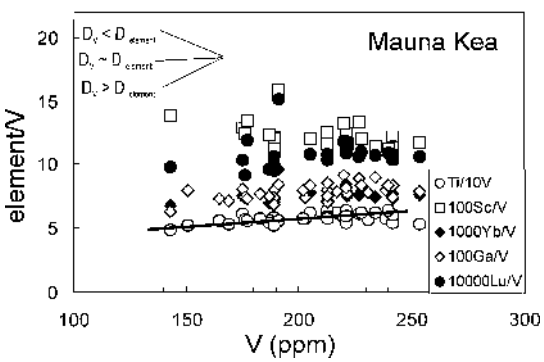

FIG. 6. (a) Covariation of Lu, Ti, Ga, Sc, Yb with V in a suite of picrites from the Mauna Kea shield intersected in the Hawaii Scientific Drillhole (Rhodes 1996, Yang *et al.* 1996). Note the differences in incompatibility of all the elements when compared to V and the interrelationship of $D_{element}^{ol/liq}$ values (upper left) required to explain the covariations. The solid line for Ti and V is calculated assuming crystal fractionation and accumulation of olivine only at NNO – 3.1, or at NNO – 2.6 with 1% chromian spinel (using $D_{element}^{ol/liq}$ from this study and $D_V^{ol/liq}$ from Canil (1999). Consideration of chromian spinel increases the $f(O_2)$ required to fit the covariation of Ti and V. Similar relationships are observed for the other elements Lu, Ga, Sc, Yb. The slopes of the covariations of Lu, Ti, Ga, Sc, Yb with V require that $D_V^{ol/liq}$ be greater than $D_{Ti,Lu,Ga,Yb}^{ol/liq}$, but less than $D_{Sc}^{ol/liq}$ during olivine sorting (see inset), and limit the $f(O_2)$ during differentiation to be between NNO – 0.5 and NNO – 3.5 (see Fig. 5b).

an $f(O_2)$ of NNO – 3.2, or at NNO – 2.1 if 1% spinel is added to the fractionating assemblage (Fig. 6). Addition of more spinel to the fractionating assemblage only serves to increase further the $f(O_2)$ required to fit the liquid line of descent. Thus consideration of olivine-only control in picrite suites, although probably not correct in detail, still provides a minimum limit for $f(O_2)$.

In the modeling shown in Figure 6, a 25% relative change in $D_{element}^{ol/liq}$ would shift the $f(O_2)$ constrained from V partitioning by ±0.5 log units. This shift represents the effect of uncertainty in the experimental data. Consideration of uncertainties in analytical data for picrite suites will increase the overall uncertainty in $f(O_2)$. Whereas the use of V partitioning and covariations with other incompatible elements is not particularly precise, it can provide important minima and maxima in petrological modeling. This is important when it is the only available technique in lava sequences in which no other redox estimate is available, such as those with altered primary mineralogy or whole-rock geochemistry.

Canil (1997) used this approach and obtained a surprisingly high $f(O_2)$ of ~NNO ± 1 for many Archean komatiite flows, but he emphasized that truly rigorous estimates of $f(O_2)$ required improved measurements of $D_{Ti,Sc,Yb,Zr}^{ol/liq}$ in melts of the same composition as those in which $D_V^{ol/liq}$ was measured, as well as higher-quality geochemical and better spatial sampling of komatiite flows. Recent detailed sampling and geochemical data for a komatiite flow from Pyke Hill in Munro Township, Ontario (Fan & Kerrich 1997) are shown in Figure 7, and display an optimal example of this approach. The variation of Ti, Sc, Yb and Zr with V in this flow, if attributed to olivine sorting, shows that $D_V^{ol/liq}$ was equal to $D_{Ti,Yb}^{ol/liq}$ but greater than $D_{Zr}^{ol/liq}$, so a *minimum* $f(O_2)$ between NNO – 0.5 and NNO + 0.7 is required (Fig. 5b). Recall that consideration of liquidus chromian spinel will only serve to raise this estimate of $f(O_2)$. Geochemical data for Fred's Flow, a thick flow of komatiitic basalt in Munro Township, Ontario (Arndt & Nesbitt 1992), requires $D_V^{ol/liq} \approx D_{Ti}^{ol/liq}$, consistent with an $f(O_2)$ of ~NNO – 0.5 (Fig. 8). The $f(O_2)$ for both of these flows is better constrained than the earlier estimates of Canil (1997) and add more credence to the idea that at least some Archean komatiitic lavas are more oxidized than formerly appreciated in discussions of the origin and evolution of these important rocks. Further high-quality analyses from other Archean terranes will be required to evaluate the global significance of these observations.

In addition, the technique may have some application in the interpretation of redox states for extraterrestrial magmas. Data for an olivine basalt suite from the Apollo 12 site (Lofgren & Lofgren 1981) are shown in Figure 9. Textural observations suggest that samples from this suite represent the basal portion of a cooling unit that differentiated by simple settling of olivine (Papike *et al.* 1999). Assuming sorting of olivine crystals, the geochemical variation in Sc in these rocks requires that $D_V^{ol/liq}$ was greater than $D_{Sc}^{ol/liq}$ (Fig. 9), so that a *maximum* $f(O_2)$ of NNO – 3.5 is consistent with the geochemical data (Fig. 5b). A minimum $f(O_2)$ for these and other reduced lunar lavas can be attained by comparisons of V with Mn, because $D_{Mn}^{ol/liq}$ is greater than $D_{Sc}^{ol/liq}$, and will constrain the maximum $D_V^{ol/liq}$ value (see Fig. 5b). Comparison of V, Sc and Mn in this suite requires an $f(O_2)$ between NNO – 3.5 and NNO – 6, broadly consistent with the conditions inferred for many other lunar mare basalts (O'Neill 1991).

Inspection of Figure 5b reveals that the intercomparison of $D_V^{ol/liq}$ with $D_{Ti,Sc,Ga,Yb}^{ol/liq}$ allows one to constrain rather well the $f(O_2)$ for picrite suites between NNO + 0.7 and NNO – 0.5, but there is a gap in compa-

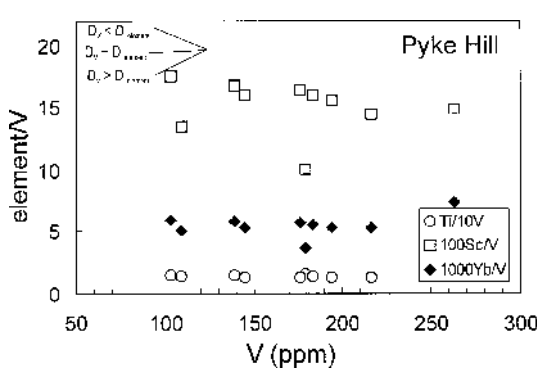

FIG. 7. Covariation of Ti, Zr, Sc, and Yb with V in a komatiite flow at Pyke Hill, Munro Township, Ontario (Fan & Kerrich 1997). During differentiation, $D_V^{ol/liq}$ is equal to $D_{Ti,Yb}^{ol/liq}$, requiring an $f(O_2)$ of ~NNO – 0.5 (see Fig. 5b).

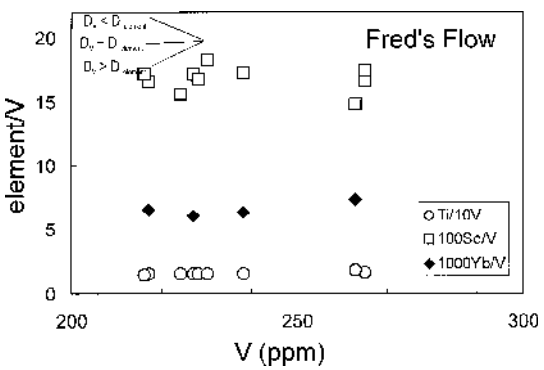

FIG. 8. Covariation of Ti, Zr, Sc and Yb with V in Fred's Flow, a layered komatiitic basalt flow in Munro Township, Ontario (Arndt & Nesbitt 1992). During differentiation, $D_V^{ol/liq}$ is equal to $D_{Ti,Yb}^{ol/liq}$, so $f(O_2)$ must have been between NNO – 0.5 and NNO + 0.7 (see Fig. 5b).

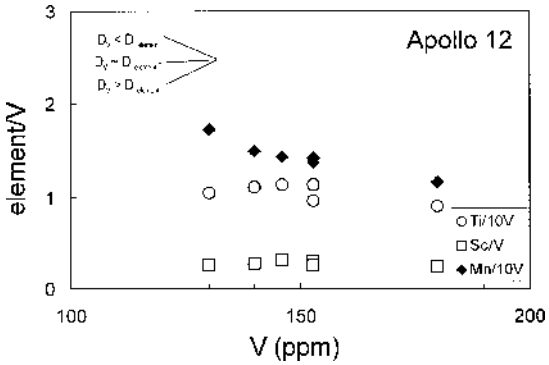

FIG. 9. Covariation of Mn and Sc with V in a suite of picrites from the Apollo 12 site (Lofgren & Lofgren 1981). For these rocks, $D_V^{ol/liq}$ is less than $D_{Mn}^{ol/liq}$ and greater than $D_{Sc}^{ol/liq}$, requiring $f(O_2)$ during differentiation to have been between NNO – 3.5 and NNO – 6 (see Fig. 5b).

rable $D_V^{ol/liq}$ values for any $f(O_2)$ between NNO – 0.5 ($D_{Ti,Yb}^{ol/liq}$) and NNO – 3.5 ($D_{Sc}^{ol/liq}$).This is the range in $f(O_2)$ observed for many modern terrestrial lavas (Carmichael 1991). Further constraints on $f(O_2)$ in this range require comparisons of V with an element having $D_{element}^{ol/liq}$ between that of Ti (0.01) and Sc (0.2). Some elements that have $D_{element}^{ol/liq}$ in this range are Lu (0.039), which was applied in the Mauna Kea suite (Fig. 6), and Ge (0.097), Cu (<0.1), Mo(0.06), Sn (0.12) and Sb (0.3). Unfortunately, the latter four elements are quite chalcophile, and could be affected by either coexisting sulfide or post-eruptive alteration. Moreover, concentrations of these elements, as well as of Ge, are almost never measured in terrestrial suites, and their geochemical behavior in magmas is not well known. As shown for the Apollo 12 suite, Mn can provide a useful constraint on magmas that crystallize at an $f(O_2)$ near the IW buffer, such as lunar and other extraterrestrial igneous rocks.

In the future, analyses of samples for these elements may help to advance the empirical approach developed in this study to constrain the $f(O_2)$ of picritic magmas in the geological record. Although uncertainties in the method are significant, crucial estimates of the minimum $f(O_2)$ can be made to test hypotheses for the origin and evolution of many terrestrial and extraterrestrial picritic rocks, to which more conventional methods of oxygen barometry cannot be applied.

ACKNOWLEDGEMENTS

We sincerely thank Peter Roeder for writing inspiring papers for us to read and try to emulate. We thank Lang Shi for assistance with the electron microprobe analyses, and Zhongxing Chen for help with the LA–ICP–MS instrumentation. Reviews by an anonymous referee, Robert F. Martin, and especially Jon Blundy greatly helped in the presentation of this paper. This research was supported by NSERC research and equipment grants to DC. The UVic LA–ICP–MS facility is supported by NSERC Major Equipment grants.

REFERENCES

ARNDT, N. & NESBITT, R.W. (1992): Geochemistry of Munro Township basalts. In *Komatiites* (N. Arndt & R.W. Nesbitt, eds.). Allen and Unwin, New York, N.Y. (309-329).

BAKER, M.B., ALVES, S. & STOLPER, E.M. (1996): Petrography and petrology of the Hawaii Scientific Drilling Project lavas: inferences from olivine phenocryst abundances and compositions. *J. Geophys. Res.* **101**, 11715-11728.

BARNES, S.J. (1986): The distribution of chromium among orthopyroxene, spinel and silicate liquid at atmospheric pressure. *Geochim. Cosmochim. Acta* **50**, 1889-1909.

BEATTIE, P. (1994): Systematics and energetics of trace element partitioning between olivine and silicate melts: implications for the nature of mineral/melt partitioning. *Chem. Geol.* **117**, 57-71.

BLUNDY, J.D. & WOOD, B.J. (1994): Prediction of crystal–melt partition coefficients from elastic moduli. *Nature* **372**, 452-454.

BORISOV, A.A., KADIK, A.A., ZHARKOVA, Y.V. & KALINICHENKO, N.V. (1988): Effects of oxygen fugacity on the ratio between valency forms of vanadium in magmas. *Geochem. Int.* **24**, 15-20.

BOWEN, N.L. (1928): *The Evolution of the Igneous Rocks*. Dover Publications Inc., New York, N.Y.

CANIL, D. (1997): Vanadium partitioning and the oxidation state of Archean komatiite magmas. *Nature* **389**, 842-845.

_____ (1999): Vanadium partitioning between orthopyroxene, spinel and silicate melt and the redox states of mantle source regions for primary magmas. *Geochim. Cosmochim. Acta* **63**, 557-572.

_____ & FEDORTCHOUK, Y. (2000): Clinopyroxene–liquid partitioning for vanadium and the oxygen fugacity during formation of cratonic and oceanic mantle lithosphere. *J. Geophys. Res.* **105**, 26003-26016.

CARMICHAEL, I.S.E. (1991): The redox states of basic and silicic magmas: a reflection of their source regions? *Contrib. Mineral. Petrol.* **106**, 129-141.

CHEN, ZHONGXING (1999): Inter-element fractionation and correction in laser ablation inductively coupled plasma mass spectrometry. *J. Anal. Atom. Spec.* **14**, 1823-1828.

_____, CANIL, D. & LONGERICH, H.P. (2000): An automated method for in situ laser ablation ICP MS analysis. *Fresenius J. Anal. Chem.* **368**, 73-78.

COLSON, R.O., MCKAY, G.A. & TAYLOR, L.A. (1988): Temperature and composition dependencies of trace element partitioning: olivine/melt and orthopyroxene/melt. *Geochim. Cosmochim. Acta* **52**, 539-553.

FAN, J. & KERRICH, R. (1997): Geochemical characteristics of aluminum depleted and undepleted komatiites and HREE-enriched low Ti tholeiites, western Abitibi greenstone belt: a heterogeneous mantle plume – convergent margin environment. *Geochim. Cosmochim. Acta* **61**, 4723-4744.

FRANCIS, D. (1995): Implications of picritic lavas for the mantle sources of terrestrial volcanism. *Lithos* **34**, 89-105.

GAETANI, G.A. & GROVE, T.L. (1997): Partitioning of moderately siderophile elements among olivine, silicate melt, and sulfide melt: constraints on core formation in the earth and Mars. *Geochim. Cosmochim. Acta* **61**, 1829-1846.

HART, S.R. & DAVIS, K.E. (1978): Nickel partitioning between olivine and silicate melt. *Earth Planet. Sci. Lett.* **40**, 203-219.

HIRSCHMANN, M. & GHIORSO, M.S. (1994): Activities of nickel, cobalt and manganese silicates in magmatic liquids and applications to olivine/liquid and silicate/metal partitioning. *Geochim. Cosmochim. Acta* **58**, 4109-4126.

KENNEDY, A.K., LOFGREN, G.E. & WASSERBURG, G.J. (1992): An experimental study of trace element partitioning between olivine, orthopyroxene and melt in chondrules: equilibrium values and kinetic effects. *Earth Planet. Sci. Lett.* **115**, 177-195.

LOFGREN, G.E. & LOFGREN, E.M. (1981): *Catalog of Lunar Mare Basalts Greater than 40 Grams. I. Major and Trace Chemistry*. NASA, Houston, Texas.

O'NEILL, H.S.C. (1991): The origin of the Moon and the early history of the Earth – a chemical model. 1. The Moon. *Geochim. Cosmochim. Acta* **55**, 1135-1157.

ONUMA, N., HIGUCHI, H., WAKITA, H. & NAGASAWA, H. (1968): Trace element partition between two pyroxenes and the host lava. *Earth Planet. Sci. Lett.* **5**, 47-51.

PAPIKE, J.J., FOWLER, G.W., ADCOCK, C.T. & SHEARER, C.K. (1999): Systematics of Ni and Co in olivine from planetary melt systems: lunar mare basalts. *Am. Mineral.* **84**, 392-399.

RHODES, J.M. (1996): Geochemical stratigraphy of lava flows sampled by the Hawaii Scientific Drilling Project. *J. Geophys. Res.* **101**, 11729-11747.

ROEDER, P.L. & EMSLIE, R.F. (1970): Olivine–liquid equilibrium. *Contrib. Mineral. Petrol.* **29**, 275-289.

_____ & REYNOLDS, I. (1991): Crystallization of chromite and chromium solubility in basaltic melts. *J. Petrol.* **32**, 909-934.

RUBIE, D.C., KARATO, S., YAN, H. & O'NEILL, H.S. (1993): Low differential stress and controlled chemical environment in multianvil high-pressure experiments. *Phys. Chem. Minerals* **20**, 315-322.

SCHREIBER, H.D. & HASKIN, L.A. (1976): Chromium in basalts: experimental determination of redox states and partitioning among synthetic silicate phases. *Proc. Lunar Planet. Sci. Conf.* **7**, 1221-1259.

SHANNON, R.D. (1976): Revised effective ionic radii and systematic studies of interatomic distances in halides and chalcogenides. *Acta Crystallogr.* **A32**, 751-767.

SNYDER, D.A. & CARMICHAEL, I.S.E. (1992): Olivine–liquid equilibria and the chemical activities of FeO, NiO, Fe_2O_3, and MgO in natural basic melts. *Geochim. Cosmochim. Acta* **56**, 303-318.

SUZUKI, T. & AKAOGI, M. (1995): Element partitioning between olivine and silicate melt under high pressure. *Phys. Chem. Minerals* **22**, 411-418.

TAKAHASHI, E. (1978): Partitioning of Ni, Co, Fe, Mn and Mg between olivine and silicate melts: compositional dependence of partition coefficient. *Geochim. Cosmochim. Acta* **42**, 1829-1844.

VON SECKENDORFF, V. & O'NEILL, H.ST.C. (1993): An experimental study of Fe–Mg partitioning between olivine and orthopyroxene at 1173, 1273 and 1423 K and 1.6 GPa. *Contrib. Mineral. Petrol.* **113**, 196-207.

WEBB, S.L. & DINGWELL, D.B. (1990): Non-Newtonian rheology of silicate melts at high stresses and strain rates: experimental results for rhyolite, andesite, basalt and nephelinite. *J. Geophys. Res.* **95**, 15695-15702.

WOOD, B.J. & BLUNDY, J.D. (1997): A predictive model for rare earth element partitioning between clinopyroxene and anhydrous silicate melt. *Contrib. Mineral. Petrol.* **129**, 166-181.

YANG, H.J., FREY, F.A., RHODES, J.M. & GARCIA, M.O. (1996): Evolution of the Mauna Kea volcano: inferences from lava compositions recovered in the Hawaii Scientific Drilling Project. *J. Geophys. Res.* **101**, 11747-11768.

Received December 20, 1999, revised manuscript accepted October 15, 2000.